NASA-CR-203246

AIAA-96-3391

Natural Rolling Responses of a Delta Wing in Transonic and Subsonic Flows

M. Menzies and O. Kandil
Old Dominion University
Norfolk, VA

AIAA Atmospheric Flight Mechanics Conference
July 29-31, 1996 / San Diego, CA

NATURAL ROLLING RESPONSES OF A DELTA WING IN TRANSONIC AND SUBSONIC FLOWS

Margaret A. Menzies† and Osama A. Kandil‡
Aerospace Engineering Department
Old Dominion University, Norfolk, Virginia 23529

ABSTRACT

The unsteady, three-dimensional, full Navier-Stokes (NS) equations and the Euler equations of rigid-body dynamics are sequentially solved to simulate the natural rolling response of slender delta wings of zero thickness at moderate to high angles of attack, to transonic and subsonic flows. The governing equations of fluid flow and dynamics of the present multi-disciplinary problem are solved using the time-accurate solution of the NS equations with the implicit, upwind, Roe flux-difference splitting, finite-volume scheme and a four-stage Runge-Kutta scheme, respectively. The main focus is to analyze the effect of Mach number and angle of attack on the leading edge vortices and their breakdown, the resultant rolling motion, and overall aerodynamic response of the wing. Three cases demonstrate the natural response of a 65° swept, cropped delta wing in a transonic flow with breakdown of the leading edge vortices and an 80° swept delta wing in a subsonic flow undergoing either damped or self-excited limit-cycle rolling oscillations as a function of angle of attack. Comparisons with an experimental investigation completes this study, validating the analysis and illustrating the complex details afforded by computational investigations.

INTRODUCTION

The concept of aircraft "supermanuerverability" introduced in the early 1980's has inspired a great deal of research on high angle of attack maneuvering through control of unsteady vortical flowfields. The ability to accurately predict the time-dependent flowfield and dynamic response of an aircraft is essential to insure the integrity and safety of the vehicle. Additionally, better understanding of the unsteady and separated flows associated with oscillating delta wings must be developed to exploit these flight regimes and extend current performance envelopes in the transonic regime.

For both forced pitching and rolling delta wings, Nelson and his co-authors have performed numerous experimental investigations. Pelletier and Nelson[1] studied static and dynamic pitching and rolling of a 65° swept delta wing. They concluded: for dynamic constant amplitude motions, both in pitch and roll, breakdown is affected by the reduced frequency; increases in the width of the hysteresis loop and the time lag corresponds to increasing the reduced frequency of oscillation; and in roll, the leeward side of the wing has breakdown downstream of the windward side. They also stated that it appears that rolling a wing influences breakdown because it modifies the effective angle of attack and the effective sweep angle[1].

Additional forced rolling oscillation investigations were performed by Ericsson and Hanff[2]. They analyzed experimental results of a rolling 65° swept delta wing at 30° angle of attack to try to determine the fluid mechanism causing the "unusual, highly nonlinear vehicle dynamics." They concluded: static and dynamic roll characteristics are largely determined by the effect of vortex breakdown; the dynamic effect of vortex breakdown is to a large extent controlled by the roll-rate-induced conical camber; and, the roll response to both roll angles and roll rate are subject to significant convective time-lag effects. Meanwhile, Hanff and Huang[3] attempted to develop a method to predict the unsteady loads acting on the delta wing undergoing an arbitrary motion. The aim of these forced motion investigations was to suggest aerodynamic characteristics which may account for the limit cycle oscillation known as wing rock.

In 1981, the phenomena of slender wing rock was first observed in experiments performed by Nguyen, *et al*[4]. Using an 80° swept delta wing investigation showed that wing rock occurred simultaneously with the appearance of asymmetric leading-edge vortices. By 1984, Ericsson[5] had shown that vortex asymmetry could generate wing rock but growth of the amplitude was limited by vortex breakdown. Under the advisement of Nelson, Arena[6] conducted a thorough experimental investigation of the natural response of a slender wing rock in subsonic flow. He identified the envelope of damped and self sustaining motion for an 80° swept wing. Furthermore, he hypothesized that vortex breakdown limits the steady state amplitude of the wing rock. Above an angle of attack which promotes vortex breakdown, the limit cycle amplitude becomes chaotic with non-periodic fluctuations. Continuing investigation of wing rock, Ng, *et al.*,[7] used a water tunnel to compare forced rolling and free-to-roll oscillations of delta wings of various sweep angles with static conditions. Their results showed that the wing rock can occur in the absence of asymmetric vortex lift-off, vortex breakdown, and static hysteresis. From this, they concluded that these flow phenomena are not necessary for wing rock to occur. However, their presence in the flowfield can have strong influence on the amplitude and frequency of the limit cycle. This observation was further substantiated by Ericsson, "Analysis of experimental results for slender delta wings reveals that asymmetric lift-off of the leading-edge vortices on slender delta wings does not start the wing rock, although it is responsible for the large limit cycle amplitude observed in experiments."[8].

Computational investigations of delta wings oscillating in roll were initiated by Kandil, *et al*,[9] in 1978 using a nonlinear discrete-vortex method. In 1988, Kandil and Chuang[10] solved for a locally conical supersonic flow over a sharped-edged delta wing at zero angle of attack using unsteady Euler equations. The Euler equations were formulated using a moving frame of reference which were solved by using an explicit, multi-staged, time-accurate, finite-volume scheme. The

†Graduate Research Assistant, Member AIAA.

‡Professor, Eminent Scholar and Department Chairman, Associate Fellow AIAA.

results showed detailed formation, interaction, and disappearance of the primary vortex and shock. A complete review of this work is found in Chuang's dissertation[11]. In later papers, to improve their model, Kandil and Chuang[12, 13, 14] proceeded to solve for supersonic flow over rolling delta wings, using thin-layer Navier-Stokes Equations written in the moving frame of reference. Assuming locally conical flow, both a sharp-edged and rounded-edged wings, held at a mean angle of attack of 10°, were oscillated ± 15° at a Reynolds number of 0.5 x 10^6 and Mach number of 2.0. The time history of lift and rolling moment coefficients were presented along with computed flow characteristics which described the behavior of the primary vortex and shock waves.

Subsonic flow over a rolling delta wing was computed in 1992, by Chaderijian,[15, 16] using the full three-dimensional Reynolds-averaged, Navier-Stokes equations. Using a 65° swept delta wing undergoing static roll and large-amplitude high-rate-of-roll oscillations, Chaderjian studied the effects of grid refinement and roll angle on the breakdown free vortex aerodynamics. He concluded that the static rolling-moment characteristics indicated that the wing is statically stable. The dynamic rolling-moment coefficient indicated that the fluid extracts energy from the wing motion indicating that the wing was positively damped. He also noted that there were significant rate-induced time-history lags in the rolling-moment coefficient but negligible lags in the normal-force coefficient and center-of-pressure position. Lastly, comparison with experimental results showed that a medium density grid provided sufficient resolution of the pertinent flow physics. In 1993, Gordnier and Visball[17] studied the flowfield around an 80° swept delta wing undergoing a constant roll-rate maneuver from 0° to 45°. Using the unsteady, full, three-dimensional Navier-Stokes equations, they described the dynamical behavior of the vortices. "The right vortex (downward leading edge) moves inborad and towards the surface while the left vortex (upward leading edge) moves outboard and away from the surface. A lag in the body-normal position of the left vortex similar to the lag observed for delta wing rock was noted. The left vortex continually loses strength during the roll maneuver. The right vortex initially gains strength but then rapidly losses strength as high roll angles are achieved"[17]. They concluded that this vortex behavior was based on the effective angle of attack and sideslip angles during the rolling motion.

In the transonic regime, the only known published study of forced rolling oscillation of a delta wing was performed by Menzies, Kandil and Kandil[18] in 1995. In this study the unsteady, three-dimensional, full Navier-Stokes equations are solved for flow over a 65° sharp-edged cropped delta wing undergoing forced sinusoidal rolling oscillations of $\neq 4°$. At an angle of attack of 20° and Mach number of 0.85, the wing was oscillated at various rolling reduced frequencies and Reynolds number to observe the effect on the vortex breakdown. It was shown that as the wing rolls at a reduced frequency of 2π, an oscillatory expansion and compression of the vortex cores and breakdown occurs. Review of the instantaneous streamlines, which mark the beginning of the vortex breakdown by their disordered appearance, indicated that as the wing rolls, the breakdown washes downstream. It was surmised that when the wing rolls downward, there is a relieving effect on the transverse shock which weakens the shock, enabling the vortex core to penetrate without breakdown. After six and a half cycles of motion, a periodic solution is reached without breakdown. A significant rise in the lift coefficient is noted as a result.

In this paper, three cases demonstrate the natural rolling response of a delta wing in transonic and subsonic flow. Transonic flow over a 65° swept, cropped delta wing with breakdown of the leading edge vortices demonstrates self sustained rolling oscillations until breakdown dominates the flow field. Two cases of subsonic flow over an 80° swept wing demonstrate either damped and self-sustained rolling oscillations as a function of angle of attack. A complete investigation of the aerodynamic response of the wing, the effects of mach number, angle of attack, and vortex breakdown are presented.

FORMULATION

Governing Equations:

The conservative form of the dimensionless, unsteady, compressible, full Navier-Stokes equations in terms of the time-dependent, body-conformed coordinates ξ^1, ξ^2, and ξ^3, is given by:

$$\frac{\partial \overline{Q}}{\partial t} + \frac{\partial \overline{E}_m}{\partial \xi^m} - \frac{\partial (\overline{E}_v)_s}{\partial \xi^s} = 0; \quad m = 1,2,3; \; s = 1,2,3 \tag{1}$$

where

$$\xi^m = \xi^m(x_1, x_2, x_3, t) \tag{2}$$

$$\overline{Q} = \frac{\hat{q}}{J} = \frac{1}{J}[\rho, \rho u_1, \rho u_2, \rho u_3, \rho e]^t \tag{3}$$

The definitions of the inviscid and viscous fluxes; $\overline{E}_m$ and $(\overline{E}_v)_s$ are given in Ref. 19.

To achieve the natural response of the wing to the fluid flow, the wing motion is obtained by coupling the fluid dynamics with rigid body dynamics. The resultant external aerodynamic rolling moment, $C_{m_{roll}}$, is equated to the time rate of change of the angular momentum vector about the axis of rotation as follows:

$$C_{m_{roll}} = I_{xx}\dot{\omega}_x + (I_{zz} - I_{yy})\omega_y\omega_z \tag{4}$$

where I_{ii} are the principal mass moments of inertia for the wing, ω_x is the rolling velocity, and ω_y and $\omega_z = 0$ for single degree of freedom motion (rolling motion).

Boundary and Initial Conditions and Grid Motion:

All boundary conditions are explicitly implemented. They include inflow-outflow conditions, solid-boundary conditions and plane of geometric symmetry conditions. At the plane of geometric symmetry, periodic conditions are enforced. At the inflow boundaries, the Riemann-invarient boundary-type conditions are enforced. At the outflow boundaries, first-order extrapolation from the interior point is used.

Since the wing is undergoing rolling motion, the grid is moved with the same angular motion as that of the body. The grid speed, $\frac{\partial \xi^m}{\partial t}$, and the metric coefficient, $\frac{\partial \xi^m}{\partial x_n}$, are computed at each time step of the computational scheme. Consequently, the kinematic boundary conditions at the inflow-outflow boundaries and at the wing surface are expressed

in terms of the relative velocities. The dynamic boundary condition, $\frac{\partial p}{\partial n}$, on the wing surface is no longer equal to zero. This condition is modified for the oscillating wing as:

$$\frac{\partial p}{\partial n}\Big|_{wing} = -\rho\,\bar{a}\cdot\hat{n} \tag{5}$$

where $\bar{a}$ is the acceleration of a point on the wing flat surface; $\hat{n}$, the unit normal to the wing surface which is equal to the unit vector $\bar{e}_z$ for a flat surface. The acceleration is given by:

$$\bar{a} = \dot{\bar{\Omega}}\times\bar{r} + \bar{\Omega}\times(\bar{\Omega}\times\bar{r}) \tag{6}$$

where $\bar{\Omega}$ is the angular velocity. Notice that for a rigid body, the position vector $\bar{r}$, is not a function of time and hence, $\dot{\bar{r}} = \ddot{\bar{r}} = 0$. Finally, the boundary condition for the temperature is obtained from the adiabatic boundary condition and is given by:

$$\frac{\partial T}{\partial n}\Big|_{wing} = 0 \tag{7}$$

The initial conditions for the transonic flow case correspond to the flow solution around a stationary 65° swept, delta wing at an angle of attack of 20° that was impulsively inserted into a free stream with $M_\infty = 0.85$, and Reynolds number of 3.23 x 10^6. The solution after 18,000 time steps with a time step of $\Delta t = 0.0002$ is then used for the starting point for the transonic flow case. The initial conditions for the two subsonic cases correspond to the flow solution around a stationary wing at an angle of attack of 20°, and 30° respectively. The 80° swept, delta wing was impulsively inserted into a free stream with $M_\infty = 0.1$, and Reynolds number of 0.4 x 10^6. The solution after 17,500 time steps with a time step of $\Delta t = 0.001$ is then used for the starting point for the subsonic flow cases.

COMPUTATIONAL SCHEME

The implicit, upwind, flux-difference splitting, finite-volume scheme is used to solve the unsteady, compressible, full Navier-Stokes equations. This scheme uses the flux-difference splitting of Roe and a smooth flux limiter is used to eliminate oscillation at locations of large flow gradients. The viscous and heat flux terms are linearized in time and the cross derivative terms are eliminated in the implicit operator and retained in the explicit terms. The viscous terms are differenced using second-order accurate central differencing. The resulting difference equation is approximately factored to solve the equations in three sweeps in the ξ^1, ξ^2, and ξ^3, directions. The computational scheme is coded in the computer program "FTNS3D".

The method of solution consists of three steps. In the first step, the problem is solved for the stationary wing at 0° roll angle. This solution represents the initial conditions for the second step. In the second step, the dynamic initial conditions are specified. For the transonic case, the wing is subjected to an initial velocity. For the subsonic cases, a quarter cycle of a sinusoidal function is specified to roll the wing to a 10° roll angle with zero angular velocity while the Navier-Stokes equations are solved accurately in time. Having specified the dynamic initial conditions, the third step proceeds. Applying a four-stage Runge-Kutta scheme and the specified dynamic initial conditions for θ and $\dot{\theta}$, Eq. (4) is explicitly integrated in time in sequence with the fluid dynamic equations. Equations (4) is used to solve for θ, $\dot{\theta}$, and $\ddot{\theta}$ while the fluid dynamics equations provide the pressure distribution over the wing surface. The pressure distribution is integrated over the surface of the wing to determine $C_{m_{roll}}$, with respect to the axis of geometric symmetry. At each time step, the wing and the grid are rotated corresponding to θ and $\dot{\theta}$ resulting in the natural rolling response of the delta wing to the fluid flow. Due to the dynamic nature of the problem, the metric coefficients and the grid speed are computed at each time step. The computations proceed until periodic response is reached.

COMPUTATIONAL APPLICATION AND DISCUSSION

Case I-Transonic Flow over a 65°-Swept Cropped Delta Wing undergoing Divergent Rolling Oscillations

A 65° swept-back, sharp edged, cropped delta wing of zero thickness is considered for the transonic flow solutions. The cropping ratio (tip length/root-chord length) is 0.15. An O-H grid of 65 x 43 x 105 in the wrap-around, normal, and axial directions, respectively, is used. The computational domain extends two chord lengths forward and five chord lengths downstream of the wing trailing edge. The radius of the computational domain is four chord lengths. The minimum grid size in the normal direction to the wing surface is 5 x 10^{-4} from the leading edge to the plane of symmetry. The initial conditions correspond to the solution of the wing held at 20° angle of attack and 0° roll angle after 18,000 time steps at a Mach number and Reynolds number of 0.85 and 3.23 x 10^6, respectively.

Plots of the initial condition depict a solution characterized by weak oblique shocks beneath the primary vortices and a strong, transverse terminating shock located at approximately $x = 0.86$ (See Fig. 1). These shocks bound a substantial supersonic pocket. Outboard of the oblique shocks, a subsonic, separated region depicts a secondary vortex which exists until $x = 0.91$. The primary vortex interacts with the terminating shock and enlarges indicating vortex breakdown. The plots of the Mach number contours, instantaneous streamlines, and surfaces of constant entropy shown in Figure 1 depict clearly a bubble type vortex breakdown and the flow appears to be completely symmetric. Additional details of this flow solution along with comparisons with experimental data are shown in Ref. 19.

From the initial conditions, the wing is given an instantaneous roll velocity of $\dot{\theta} = +0.925$ x 10^{-4}. For convention, a positive roll velocity indicate that the right hand side of the wing when looking in the upstream direction is moving upward. With a dimensionless mass moment of inertia of $I_{xx} = 2.88$ x 10^{-3}, the wing is free to respond to the rolling moment induced by the fluid flow. Figure 2 shows the time history of the resultant motion and lift coefficient curve. While the motion appears somewhat periodic after $t = 30$, there is a chaotic behavior in the cyclic response due to the vortex breakdown which leads to divergence of the motion after five cycles of rolling. The highly unsteady nature of the shock induced vortex breakdown promotes very irregular motion and aerodynamic response histories. The lift coefficient indicates an initial loss after the onset of motion and fluctuates between 0.36 and 0.40 during the quasi-periodic response. After $t = 120$ when

the wing motion diverges to approximately 24°, the lift drops considerably.

Figure 3 shows snapshots of the Mach contours near the wing surface and surfaces of constant entropy depicting the primary vortex core and breakdown. During the quasi-periodic response, the terminating shock and vortex breakdown location oscillate laterally as shown in views a) to d). In contrast to subsonic flow where the breakdown and restructuring of the vortex serves to dampen the motion;[6] in transonic flow, the sustained oscillation of the wing appears to be caused by the asymmetric motion of the breakdown location. However, as time progresses, the frequency of oscillation is slightly increased. In Ref. 18, it was shown that when forced to roll at a reduced frequency of 2π, the transverse shock was weakened as a result of the motion and the breakdown washes downstream. In this case, after $t = 120$, (shown in view e), the shock on the upward moving side appears to weaken as a result of the increased rolling frequency and the breakdown washes downstream. On the downward moving side, the breakdown location advances to the apex of the wing which results in a significant drop in the lift. Without breakdown on the right side, the wing rolls until equilibrium is reached at a positive mean roll angle of 24.2°. Small amplitude fluctuations of this roll angle are observed due to the unsteady nature of the complete breakdown on the left side of the wing.

Case II-Subsonic Flow over an 80°-Swept Delta Wing undergoing Damped Rolling Oscillations

In order to compare with available experimental data, an 80° swept-back, sharp-edged delta wing of zero thickness is considered for the subsonic flow solutions. This wing was modeled after the experimental model used by Arena[6]. An O-H grid of 65 x 43 x 84 in the wrap-around, normal, and axial directions, respectively, is used. The computational domain extends two chord lengths forward and five chord lengths backward from the wing trailing edge. The radius of the computational domain is four chord lengths. The minimum grid size in the normal direction to the wing surface is 5 x 10^{-4} from the leading edge to the plane of symmetry. The initial conditions correspond to the solution of the wing held at 10° angle of attack and 0° roll angle after 17,500 time steps at a Mach number and Reynolds number of 0.1 and 0.4 x 10^6, respectively. The flowfield has no observable vortex breakdown.

From the initial conditions, the wing is forced to roll to an initial roll angle of $\theta = 10.0°$. Again, by convention, a positive roll angle indicates that the right hand side of the wing when looking in the upstream direction is rolled upward. The wing is then released to respond to the fluid flow with a mass moment of inertial about the x – axis of $I_{xx} = 2.253 \times 10^{-2}$. Figure 4 shows the time history of the resultant motion and lift coefficient curve. This plot characterizes the damped rolling oscillations observed of wing at relatively low angles of attack in a subsonic freestream. At an angle of attack of 10° and $M_\infty = 0.1$, and 80° swept delta wing will not undergo self sustained wing rock. From the initial displacement of 10° roll angle, the wing rolls to a minimum of – 3.11° in overshoot and returns to a positive roll angle before reaching the steady state response at $\theta = 0°$. Meanwhile, the lift coefficient increases by 8.4%.

Figure 5 shows a comparison of the Mach number contours and instantaneous streamlines of the initial conditions when the wing is released at $\theta = 10°$ and the steady state response when the wing is at rest at $\theta = 0°$. Notice that there is very little motion of the vortex cores. As a result, the variation of the pressure distribution is extremely small. Without large pressure differences between the left and right sides of the wing, the angular velocity remains small and the motion of the wing subsides. There is no noticeable lagging of the motion of the fluid with respect to the motion of the wing.

Case III-Subsonic Flow over an 80°–Swept Delta Wing undergoing Self-sustained Rolling Oscillations

The same 80° swept-back, sharp-edged delta wing of zero thickness is considered for this case. To duplicate the experimental investigation by Arean[6], the initial conditions correspond to the solution of the wing held at 30° angle of attack and 0° roll angle after 17,500 time steps at a Mach number and Reynolds number of 0.1 and 0.4 x 10^6, respectively.

From the initial conditions, this wing is also forced to roll to an initial roll angle of $\theta = 10.0°$ as in the previous case. The wing is then released to respond to the fluid flow with a mass moment of inertial about the $x-$ axis of the $I_{xx} = 2.253 \times 10^{-2}$. Figure 6 shows the phase and time history of the resultant motion. From the initial displacement of $\theta = 10°$, the wing oscillated in roll with a growing amplitude until periodicity is reached three cycles later. By $t = 60$, the motion is completely periodic with a maximum limit-cycle amplitude of 41.2°. For comparison, the experimental results for the same wing performed by Arena[6] showed a steady state amplitude of 41° at the same Reynolds number. Viewing the time histories of all three rotational properties, it is clear that the angular acceleration and roll angle are exactly 180° out of phase, while the angular velocity is nearly 90° out of phase.

Figure 7 shows the time history of the lift coefficient and the phase of the periodic response of the rolling moment coefficient. Notice that the lift coefficient curve oscillates at twice the frequency of the wing motion. In the phase plot of the rolling moment coefficient, it is interesting to note the three lobes of the periodic response. These lobes represent the energy shift from the wing to the fluid in the outer two lobes as indicated by the "+" and from the fluid to the wing in the middle lobe as indicated by the "–". These outer lobes are referred to as damping lobes. In the plot of the time history of the angular acceleration (Fig. 6), irregularities due to the damping lobes are noted near the peaks of the curve. Since these lobes are not present in the damped oscillation case, careful study of the flowfield at these points may provide insight into the wing rock phenomenon.

Figure 8 shows snapshots of a complete cycle of rolling depicting the total pressure contours at key points labeled in Figs. 6 and 7. As the wing is approaching the maximum angular velocity, points g) to h) and j) to k), the footprint of the vortex core on the upward moving side appears to bow outward toward the leading edge of the wing. It appears that the uneven movement of the vortex core with respect to the leading edge is a result of the lagging movement of the fluid in response to the motion of the wing. Near the trailing edge, this effect is more pronounced due to the increased absolute velocity of the wing near the outer edges of the surface. When the fluid

motion catches up to the motion of the wing, the energy flows from the fluid to the wing promoting the rolling motion, and stimulating wing rock. As the wing rolls, the angular velocity increases until the wing exceeds $\theta = \pm 27°$. Near the trailing edge, the absolute velocity of the wing exceeds the limit of the motion that the fluid can maintain. The flowfield reflects this lag by the bowed appearance of the vortex core. When the fluid flow motion lags the wing motion, energy is absorbed by the fluid providing damping to the system as indicated by the "+" in rolling moment phase diagram of Fig. 7. As the wing slows, the cores appear to straighten and snap back. This effectively rolls the wing in the opposite direction.

In Figure 9, a plot of the core positions at $x = 0.77$ is shown to demonstrate the symmetric motion of the vortex cores. Note that the cubic splines connecting the individual points do not represent the path taken but are merely shown for connectivity. During the energy transfer from the wing to the fluid, from points f) to g) and i) to j), the position of the vortex cores exhibits a more vertical motion. When the energy is transferred from the fluid to the wing, the position of the vortex cores shift in a lateral direction paralleling the surface of the wing. This motion is coicident with the lagging motion of the fluid with respect to the wing.

CONCLUSIONS

The unsteady, compressible, full Navier-Stokes equations are integrated time accurately using the implicit, upwind, flux-difference splitting, finite-volume scheme and are coupled sequentially to the Euler equations of rigid-body dynamics which are solved with a four-state Runge-Kutta scheme to study the unsteady transonic and subsonic flow around slender delta wings. The natural response of the wing undergoing damped, self-sustained, and divergent rolling oscillations are shown as a function of angle of attack and Mach number. Flowfield details of the leading-edge vortices and their breakdown unable to be captured by experiment have been shown.

The first case demonstrates the effects of vortex breakdown in the transonic regime. With the shock induced vortex breakdown, the derivatives of the motion and the aerodynamic properties show a very high frequency, low amplitude disturbance resulting from the shock-vortex interaction. Oscillations in the location of the shock and vortex breakdown location induces the wing to roll, however, the wing is unable to remain in a stable limit cycle. Divergence of the motion is observed when the rolling frequency is sufficient to cause the transverse shock to weaken on the upward moving side. The wing responds by continuing to roll until an equilibrium point is reached.

The second and third case are presented to provide a comparison with available experimental data. Case II demonstrates at a relatively low angle of attack, that an 80° swept delta wing will not undergo self-sustained oscillations. Within one cycle, the wing resumes the steady state position of 0° roll angle. The motion of the wing and vortex cores is very slight. With the relatively small angular velocity of the wing, the fluid motion does not lag the motion of the wing. The flowfield then dampens the wing response and prevents self-sustained oscillations.

In contrast, the third case the delta wing at an angle of attack of 30° does exhibit the self-sustained limit-cycle rolling oscillation known as wing rock. Within three cycles of oscillation, the wing motion sustains a roll amplitude of 41.2° and a period of oscillation of 23.1 nondimensional time. The phase diagram of the rolling-moment coefficient shows three distinct lobes which represent the energy shift from the fluid to the wing and vice versa. When the wing is first released to respond to the fluid, the pressure distribution shows a much stronger asymmetry than in the previous case due to the higher angle of attack, this results in a faster roll velocity. Instead of the motion damping as in the first case, the increased velocity causes the motion to overshoot. It appears that the velocity of the wing near the trailing edge exceeds the ability of the fluid to respond. Since the motion of the vortex core is inhibited near the trailing edge, the core exhibits a distinctive bowed shape. While the motion of the fluid lags the wing response, energy is stored in the vortex cores. The wing motion slows as a result of the damping provided by the energy transfer to the fluid and reverses roll direction. With the slowing of the roll rate, the motion of the fluid ceases to lag the motion of the wing. The vortex cores appear to snap back. In doing so, the energy stored in the fluid is imparted to the wing causing the roll velocity to increase. This cyclic motion builds until the energy transfer of the system is balanced and the periodic response is maintained.

ACKNOWLEDGMENT

This work is supported by the NASA-Langley Research Center under grant No. NAG-1-648 along with partial support from the Virginia Space Grant Consortium. The computational resources provided by the NAS Center at AMES and the NASA Langley Research Center are acknowledged and appreciated.

REFERENCES

[1]Pelletier, A. and Nelson, R. C., "An Experimental Study of Static and Dynamic Vortex Breakdown on Slender Delta Wing Planforms," AIAA Paper No. 94-1879-CP, 1994.

[2]Ericsson, L. E. and Hanff, E. S., "Unique High-Alpha Roll Dynamics of a Sharp-Edged 65–Deg Delta Wing," *Journal of Aircraft*, Vol. 31, No. 3, May-June, 1994.

[3]Huang, X. Z. and Hanff, E. S., "Prediction of Leading-Edge Vortex Breakdown on a Delta Wing Oscillating in Roll," AIAA Paper No. 92–2677, June, 1992.

[4]Nguyen, L. E., Yip, L. P., and Chambers, J. R., "Self Induced Wing Rock of Slender Delta Wings," AIAA Paper No. 81–1883, August, 1981.

[5]Ericsson, L. E., "The Fluid Mechanics of Slender Wing Rock," *Journal of Aircraft*, Vol. 21, No. 5, 1984, pp. 322–328.

[6]Arena, A. S., *An Experimental and Computational Investigation of Slender Wings Undergoing Wing Rock*, Ph.D. Dissertation, University of Notre Dame, April, 1992.

[7]Ng, T. T., Malcolm, G. N., and Lewis, L. C., "Experimental Study of Vortex Flows over Delta Wings in Wing-Rock Motion," *Journal of aircraft*, Vol. 29, No. 4, July-August, 1992.

[8]Ericsson, L. E., "Slender Wing Rock Revisited," *Journal of Aircraft*, Vol. 30, No. 3, May-June, 1993.

[9]Kandil, O. A., Atta, E. H., and Nayfeh, A. H., "Three Dimensional Steady and Unsteady Asymmetric Flow Past Wings

of Arbitrary Planforms," in *Unsteady Aerodynamics*, AGARD CP-227, 1978, pp. 2.1–2.19.

[10]Kandil, O. A. and Chuang, H. A., "Unsteady Vortex-Dominated Flows around Maneuvering Wings over a wide Range of Mach Numbers," AIAA Paper No. 88–0317, 1988.

[11]Chuang, H. A., *Development of Euler Schemes for Steady and Unsteady Vortex-Dominated Delta Wing Flows Including Shock Waves*, Ph.D. Dissertation, Old Dominion University, 1988.

[12]Kandil, O. A. and Chuang, H. A., "Unsteady Navier-Stokes Computations Past Oscillating Delta Wing at High Incidence," AIAA Paper No. 89–0081, January, 1989.

[13]Kandil, O. A. and Chuang, H. A., "Comparison of Unsteady Euler and Navier-Stokes Computational Results for Vortex-Dominated Flows," in *Proceedings of the Royal Aeronautical Society, London, United Kingdom*, April 18–20, 1989.

[14]Kandil, O. A. and Chuang, H. A., "Unsteady Navier-Stokes Computations Past Oscillating Delta Wings at High Incidence, *AIAA Journal*, Vol. 28, No. 9, September 1990, pp. 1565–1572.

[15]Chaderjian, N. M., "Navier-Stokes Prediction of Large-Amplitude Delta-Wing Roll Oscillations Characterizing Wing Rock," AIAA Paper No. 92-4428–CP, 1992.

[16]Chaderjian, N. M., "Navier-Stokes Prediction of Large-Amplitude Delta-Wing Roll Oscillations," *Journal of Aircraft*, Vol. 31, No. 6, December, 1994.

[17]Gordnier, R. E. and Visbal, M. R., "Numerical Simulation of Delta-Wing Roll," AIAA Paper No. 93–0554, January, 1993.

[18]Menzies, M. A., Kandil, O. A., and Kandil, H. A., "Forced Rolling Oscillation of a 65°–Delta Wing in Transonic Vortex-Breakdown Flow," AIAA Paper No. 95–1771–CP, June, 1995.

[19]Kandil, O. A. and Kandil, H. A., "Pitching Oscillation of a 65-Degree Delta Wing in Transonic Vortex Breakdown Flow," AIAA-94–1426-CP, AIAA/ASME/ASCE/AHS/ASC Structures and Structural Dynamics Conference, Hilton Head, SC, April 18-20, 1994.

Transonic Flow-Initial Conditions

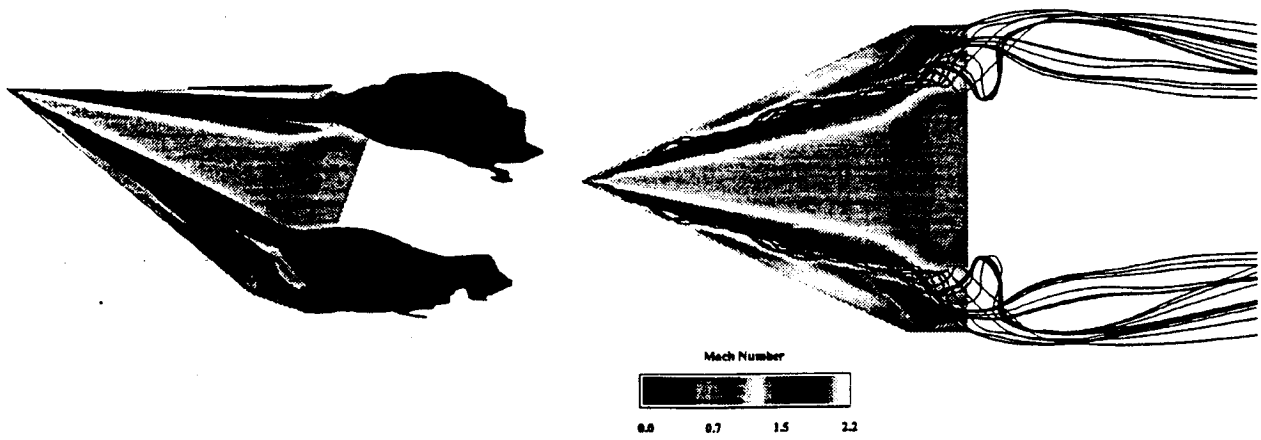

Figure 1. Mach Contours near the Wing Surface with Surfaces of Constant Entropy ($s = 0.5$) and Instantaneous Streamlines; $M_\infty = 0.85, Re = 3.23 \times 10^6, \alpha = 20.0°, \theta = 0.0°$.

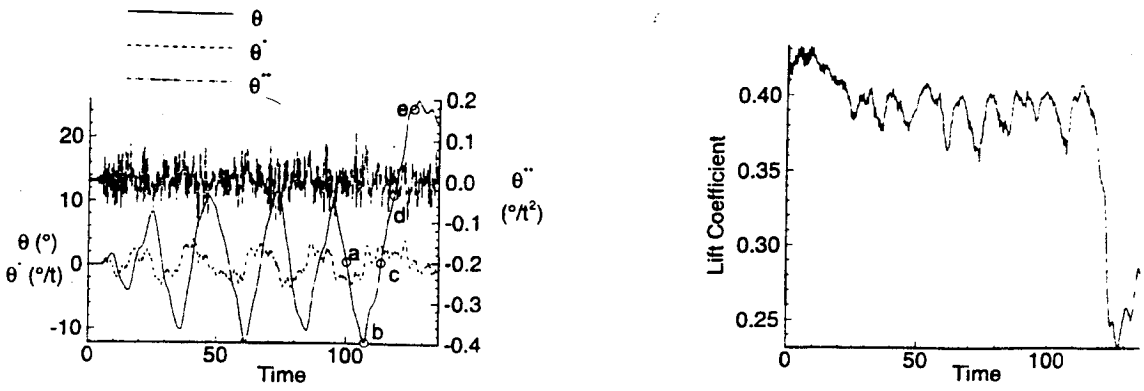

Figure 2. Time History of Roll Angle, θ, Angular Velocity, $\dot{\theta}$, Angular Acceleration, $\ddot{\theta}$, and Lift Coefficient; $M_\infty = 0.85$, $Re = 3.23 \times 10^6$, $\alpha = 20.0°$, $\theta_{ic} = 0.0°$, $\dot{\theta}_{ic} = 0.5336°/t$ (points of interest annotated).

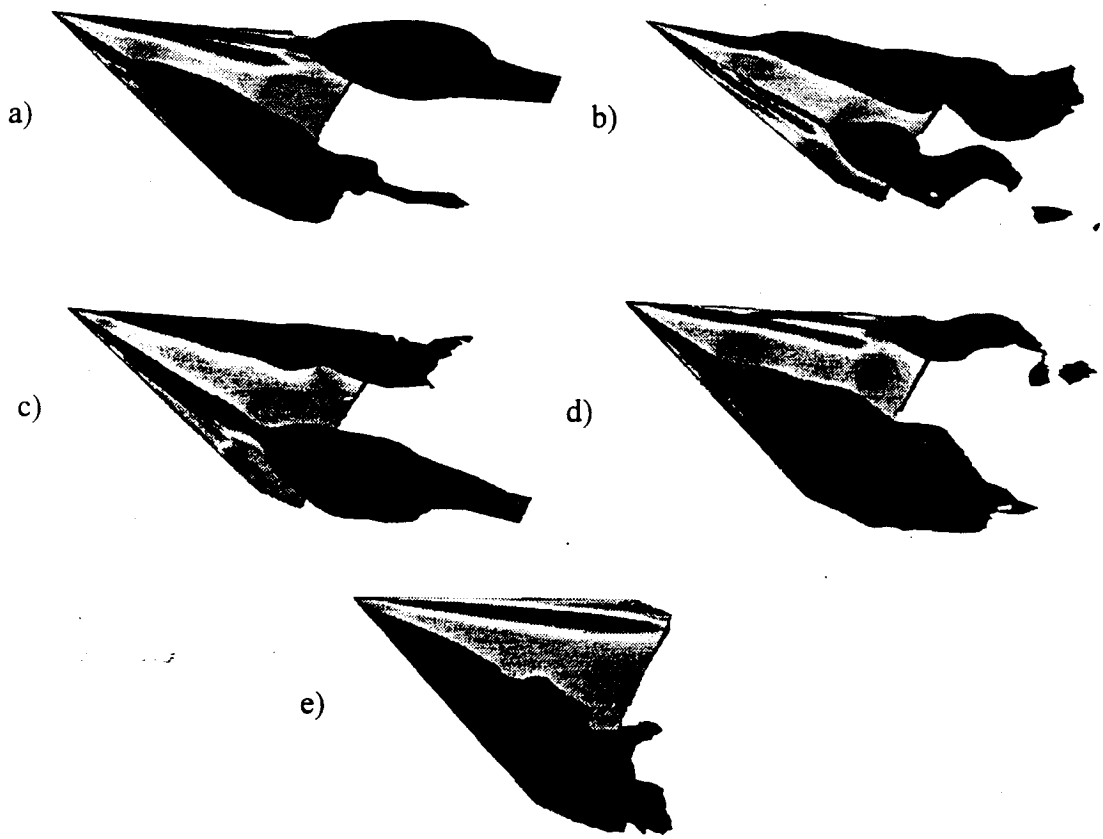

Figure 3. Snapshots of the Mach Contours near the Wing Surface with Surfaces of Constant Entropy ($s = 0.5$) at Points of Interest at a) $\theta = -0.47°$, b) $\theta = -12.10°$, c) $\theta = 0.44°$, d) $\theta = 11.08°$, e) $\theta = 24.27°$.

Subsonic Flow-Damped Oscillations

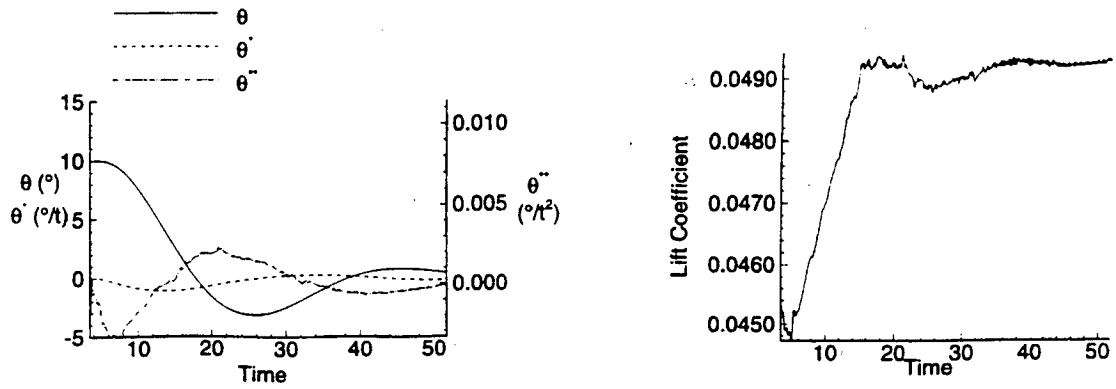

Figure 4. Time History of Roll Angle, θ, Angular Velocity, $\dot{\theta}$, Angular Acceleration, $\ddot{\theta}$, and Lift Coefficient; $M_\infty = 0.1$, $Re = 0.4 \times 10^6$, $\alpha = 20.0°$, $\theta_{ic} = 10.0°$, $\dot{\theta}_{ic} = 0.0°/t$.

$\theta = 10.0°$ $\theta = 0.0°$

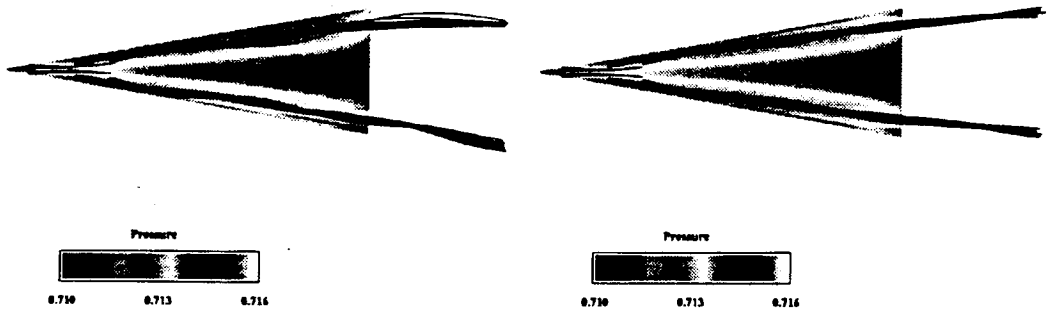

Figure 5. Comparison of Mach number Contours and Instantaneous Streamlines of Initial Conditions ($\theta = 10.0°$) and Steady State Response ($\theta = 0.0°$).

Subsonic Flow-Self-Sustained Limit-Cycle Oscillations

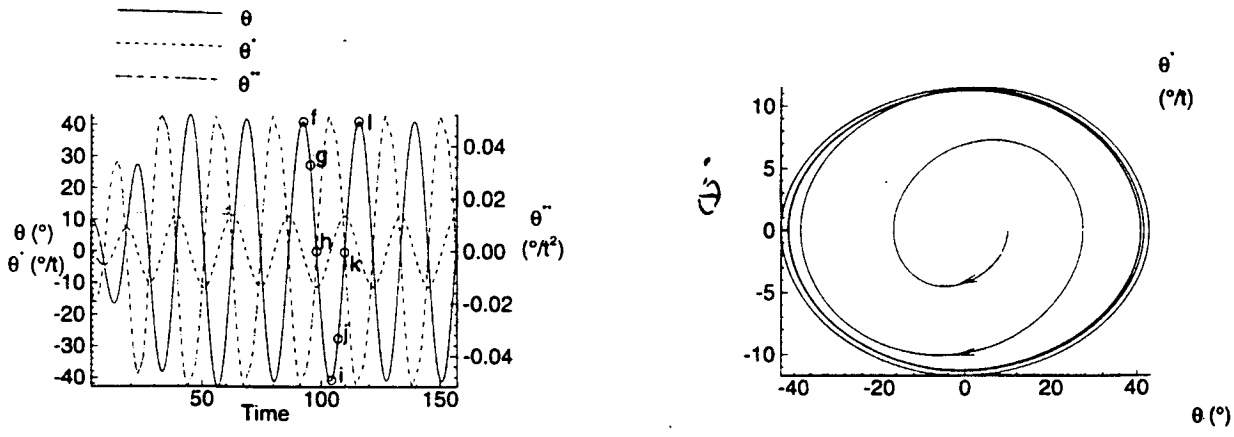

Figure 6. Time History of Roll Angle, θ, Angular Velocity, $\dot{\theta}$, Angular Acceleration, $\ddot{\theta}$ and Phase of Angular Velocity, $\dot{\theta}$; $M_\infty = 0.1$, $Re = 0.4 \times 10^6$, $\alpha = 30.0°$, $\theta_{ic} = 10.0°$, $\dot{\theta}_{ic} = 0.0°/t$ (with points of interest annotated).

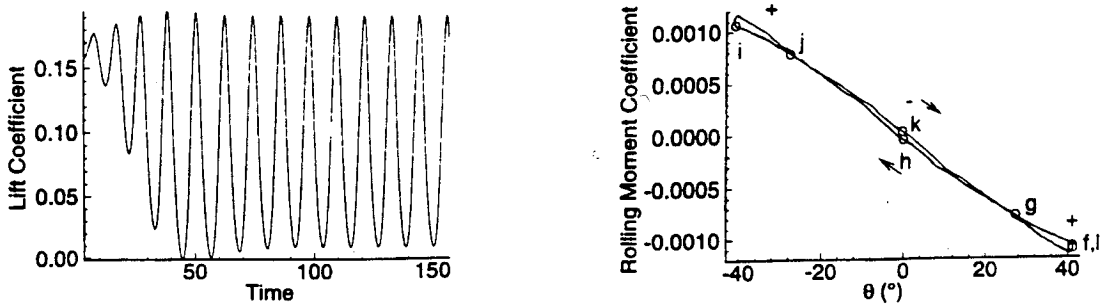

Figure 7. Time History of Lift Coefficient and Phase of Rolling Moment Coefficient indicating Energy Transfer Lobes. (with points of interest annotated).

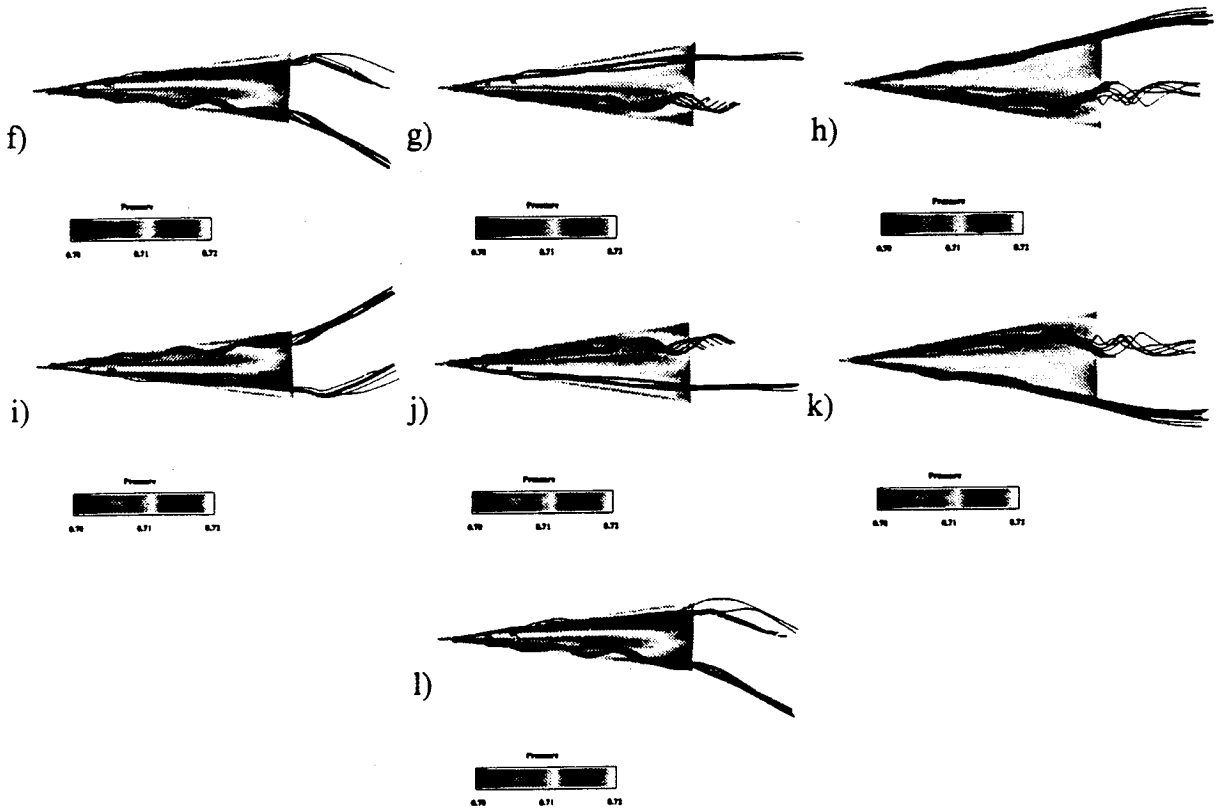

Figure 8. Snapshots of a Complete Cycle of Rolling Oscillation depicting the Total Pressure Contours at Points of Interest at $f)$ $\theta = 41.1°$, $g)$ $\theta = 27.3°$, $h)$ $\theta = 0.0°$, $i)$ $\theta = -40.8°$, $j)$ $\theta = -27.5°$, $k)$ $\theta = -0.2°$, $l)$ $\theta = 41.2°$.

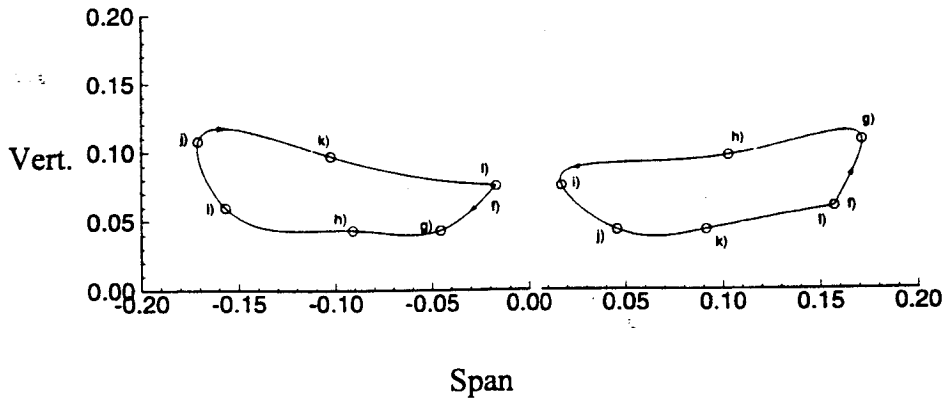

Figure 9. Plot of the Vortex Cores Positions at $x = 0.77$ at points of interest.